Journal Name

ARTICLE

Influence of isomerism on recrystallization and cocrystallization induced by CO_2 as antisolvent

C. Harscoat-Schiavo, C. Neurohr, S. Lecomte,[1] M. Marchivie[2] and P. Subra-Paternault[1]

Micronization, polymorphism, cocrystal formation are well-known strategies to modify characteristics of pharmaceutical ingredients. In this work, recrystallization induced by compressed CO2 as antisolvent was investigated as a new way to produce aminosalicylate (ASA) polymorphs and cocrystals. Three ASA isomers were first recrystallized as single species. Isomerism was particularly influent on the product characteristics. The 5-ASA isomer was produced as micrometric spherical crystals with improved flowing properties but no change of crystal lattice, 3-ASA recrystallized as micrometric spheres in a less dense crystal packing than the raw compound, and the 4-ASA isomer did not exhibit noticeable changes in morphology or crystal lattice. Cocrystallization of each isomer with nicotinamide afforded the production of ASA:NCTA cocrystal only in case of 4-ASA.

Introduction

The control of physicochemical properties of particles is a major concern for active pharmaceutical ingredients (API) since the solid-state properties deeply influence the bioavailability, hygroscopic character, stability and other performances of the drug.[1,2] Besides downsizing particles, formations of salts, polymorphs, hydrates, solvates, and more recently cocrystals are the various strategies called upon in the pharmaceutical field.[1–7] Cocrystallization is a fast-growing field with a constant identification of new cocrystals with improved physicochemical properties.[8,9]

The use of supercritical CO_2 to generate particles has been investigated for more than twenty years.[10,11] Supercritical processes offer opportunities to tune the time and space scales at which crystallization proceeds, enabling the production of new or different crystal forms or inducing more or less severe morphological changes. CO_2 has for long demonstrated its ability at micronizing organic compounds, but its capability at modifying the crystal lattice is more marginally investigated.[12–18]

[1]CNRS, CBMN, UMR 5248, Univ. Bordeaux, Bordeaux INP,F-33600 Pessac, France.
E-mail: Christelle.Harscoat-Schiavo@u-bordeaux.fr
[2]CNRS, ICMCB UPR 9048, Univ. Bordeaux, Bordeaux INP, F-33600 Pessac, France

Cocrystal formation assisted by CO_2 was only recently proposed.[19–21] A cocrystal is a molecular arrangement at solid state of two different molecules packed in periodic order through non-covalent bonds like hydrogen bonds, ion pairing, van der Waals forces, hydrophobic interactions, etc.[22–24] Although interactions are necessary to envisage cocrystal formation, they are insufficient to ensure a successful cocrystallization so various methods are to be investigated such as crystallization from solutions[25–27], grinding or melting solids[28]. Production of cocrystal by supercritical CO_2 might open interesting ways for drug delivery if for instance cocrystals can be produced at micro- or sub-micrometric scale or formulated with appropriate excipients.

In this work, the so-called GAS CO_2-antisolvent technique was investigated as a new way to produce aminosalicylate polymorphs and cocrystals. The GAS technique consists in adding compressed CO_2 to a solution that contains the species to recrystallize. The CO_2 addition induces a decrease of the solute's solubility and provokes hereafter the species precipitation. Aminosalicylic acids (fig. 1) were chosen as model compounds owing to their diverse functionalities (carboxylic acid, amine and phenol) that are favourable synthons for cocrystal formation. The three isomers, namely 5-ASA, 4-ASA and 3-ASA were processed in order to investigate the effect of isomerism upon the crystallization outcomes. 5-ASA and, to a lesser extent, 4-ASA are drugs that have been used in the treatment of ulcerative Colitis and Crohn's disease for many years.[29–31] 4-ASA itself is a well-established antibiotic used in the treatment of multiple drug-resistant tuberculosis.[32]

As for the manufacturing, 5-ASA particles are usually produced with needle-shape morphology[33], a shape generally associated to poor flow property and bulk density that induce a poor mixing with excipients.

To author's best knowledge, recrystallization of aminosalicylic acids by CO_2 technique was only attempted twice for 5-ASA.[34,35] By more conventional ways, recrystallization by evaporation was investigated for 4-ASA polymorph production[36] and for both 4-ASA and 5-ASA crystal structure packing analysis.[37] No change in the crystal form was reported. Regarding cocrystal formation, cocrystals of 4-ASA have been only recently reported.[36,38–40] No cocrystals of 5- or 3-ASA are yet described. In this work, nicotinamide (NCTA) was selected as cocrystal coformer because of its ability to form carboxyl-pyridine synthons with carboxylic acids[38] and the successful fabrication of naproxen:nicotinamide cocrystal by the CO_2-GAS technique.[19] Cocrystals and hydrates of 4-ASA:NCTA have been produced by cogrinding or evaporation[36,38] but fabrication via solution recrystallization has not been reported so far.

This work thus investigated the ability of compressed CO_2 to recrystallize aminosalicylic acids, pure or in mixture with nicotinamide, focusing on the influence of isomerism on re- and co-crystallization behaviors. It is worth noting that for 3-ASA, the crystalline structure is not yet described in the Cambridge Structural Database. Processing 4-ASA and 3-ASA with CO_2 is novelty. Regarding cocrystallization with NCTA, only cocrystals of 4-ASA are reported in literature, and they were not obtained through crystallization in solution nor by CO_2-induced precipitation. Besides crystal lattice, morphology changes and particle sizes of produced powders were documented. In case of significant size reduction, flow properties were investigated via the Carr Index and Hausner ratio.

Experimental

Materials

5-amino salicylic acid, (5-amino-2-hydroxybenzoic acid, > 99 %, 5-ASA), 4-amino salicylic acid, (4-amino-2-hydroxybenzoic acid, > 99 %, 4-ASA), 3-amino salicylic acid, (3-amino-2-hydroxybenzoic acid, 97 %, 3-ASA) and nicotinamide (pyridine-3-carboxamide, 99.5 %, NCTA) were supplied by Sigma Aldrich (France). Figure 1 shows the four molecule formulae. Carbon dioxide (CO_2, 99.5 %) was from Air Liquide (France). Acetone (99.5 %, Scharlau), DMSO (99.9 %, Scharlau), acetonitrile (HPLC grade), potassium dihydrogenophosphate and phosphoric acid were supplied by Atlantic Labo (France). Water was obtained from a Milli-Q water purification system.
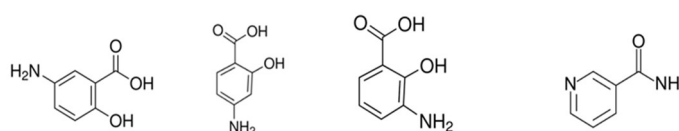
Fig. 1. Structures of the four molecules: from left to right, 5-aminosalicylic acid, 4-aminosalicylic acid, 3-aminosalicylic acid and nicotinamide. The compounds possess various functional groups that may be favourable to polymorphism and/or hydrogen bonding.

Crystallization by CO_2 antisolvent

Crystallization was carried out by the so-called GAS technique. CO_2 acts as an antisolvent, i.e. its addition to a solution provokes the precipitation of the species initially dissolved. When a mixture of API and coformer is involved (cocrystallization experiments), each compound can precipitate independently so that the produced powder is then a mixture of the two compounds in a solid state (homocrystals), or the two species can interact and form a molecular complex that precipitates in the form of cocrystals. Depending on the initial ratio of the two species, intermediary situations can occur in which cocrystals coexist with one of the homocrystals.

The experimental set-up used in this study is a home-made equipment already described.[41] Briefly, the 0.49 L vessel is equipped with a magnetically-driven impeller fit with a Rushton turbine that disperses CO_2 into the solution initially introduced in the vessel at room conditions. The vessel temperature was kept constant to 36°C and the stirring rate was set to 500 rpm. CO_2 was introduced up to 11 MPa by an ISCO pump (Model 260D, Teledyne Isco, USA) at a constant rate of 20 g/min. Once the desired pressure was attained, the formed CO_2-solvent solution that contained the non-precipitated part of solutes was withdrawn at the vessel bottom whilst fresh CO_2 flew through the vessel at 25 g/min to maintain the pressure at 11 MPa. The CO_2 flow, provided by a LEWA pump (EM1, Lewa, Germany) continued for 140 min to remove solvent traces from the vessel and precipitates. At the vessel bottom, a stainless steel filter overtopped by two 0.2 µm pore size membranes held back the produced particles whilst the solution was flushed out. Thereafter, the vessel was depressurized through the exit line and particles were collected, weighed and characterized.

API or API and coformer were dissolved in 40 mL of solvent. Due to the very different solubilities of ASA isomers, acetone or acetone: dimethyl sulfoxide mixtures were used. 5-ASA is poorly soluble in many solvents and is usually processed in dimethyl formamide (DMF) or dimethyl sulfoxide (DMSO). DMSO is a safer solvent than DMF to manipulate and is compatible with the use of CO_2 since they are miscible above a pressure of 8MPa at 35°C.[42] However, we preferred using a mixture 70:30 (vol%) of acetone (bad solvent for 5-ASA) and DMSO (good solvent) to dissolve the drug since successful CO_2 precipitation was reported with such mixture.[34,35] Moreover, with a good solvent, CO_2 as antisolvent could be not strong enough to induce the solute precipitation.[43] A lower proportion of DMSO (10%) in the acetone was also suitable to

dissolve 3-ASA without running the risk of losing the CO_2 antisolvent power. For 4-ASA, pure acetone was enough to ensure its solubilization over the investigated range of concentration. Nicotinamide, the coformer, was easily dissolved in pure acetone and in the two acetone:DMSO mixtures. Related to the solvent type, the concentration of the processed solution was varied as well depending on the ASA isomer. Table 1 summarizes the prepared solutions.

Table 1. Various solutions (solvent mixture, API and coformer concentrations) processed by the compressed CO2.

system	5-ASA	4-ASA	3-ASA	NCTA
Single species	ACE:DMSO 70:30 17 mg/ml	ACE 25 mg/ml	ACE:DMSO 90:10 14 mg/ml	ACE:DMSO 70:30 33 mg/ml
With NCTA	ACE:DMSO 70:30 API: 17 mg/ml NCTA: 17-57 mg/ml	ACE API: 25 mg/ml NCTA: 20 mg/ml	ACE:DMSO 90:10 ACE:DMSO 70:30 API: 10 mg/ml NCTA: 20 mg/ml	

Particle characterization

PARTICLE SIZE AND MORPHOLOGY The product morphology was characterized by optical microscopy (Olympus BX51TF and camera ColorView U-CMAD3) and by scanning electron microscopy SEM (JEOL 6490LV, Tokyo, Japan; accelerating voltage of 5 kV) with Au/Pd coating to induce electric conductivity on the surface of the sample (JEOL ion puttering). The particle size distribution (PSD) was measured by laser diffraction using a Mastersizer 2000 (Malvern) equipped with low volume circulation unit and using silicon oil as dispersion medium. The polydispersity, expressed by span, is calculated as: span = $(d_{90}-d_{10})/d_{50}$
in which d_{10}, d_{50} and d_{90} are the sizes corresponding to percentiles of 10%, 50% and 90% of the cumulative volume distribution.

FLOWABILITY The powder flowability was characterized by the Carr Index (CI) and the Hausner ratio (H) which are both widely used in industries as indicators of flow properties. The Carr Index and the Hauser ratio are calculated by Eq. 1 and 2, respectively, in which BD and TD are the powder bulk density and tapped density, respectively. The bulk density was calculated by loading powder in a 2 mL vial and weighing the corresponding mass. The vial was then tapped in a flat shaker (HS250 Janke & Kunkel, IKA) at 300 vibrations per minute for 3 hours to ensure no more change in the volume of powder. The measurements were carried out in triplicate (n=3).

CI (%) = (TD-BD)/TD x 100   (1)
H = TD/BD   (2)

POWDER X-RAY DIFFRACTION Crystallinity and phase identification were obtained by powder X-ray diffraction analysis (PXRD) performed on a PANalytical XPERT-PRO diffractometer equipped with a graphite monochromator, using Cu-Kα radiation (λ=1.5418 Å). The samples were deposited on a stainless steel or silicium holder. Some samples were ground to avoid preferred orientation, but PXRD patterns were first obtained without grinding to control the absence of any crushing effect. Diffraction patterns were collected for 2θ angles of 4-38° with a step size of 0.0167° at scan rate of 0.15°/min. Olex2 software was used for the preparation of

crystal structure images[44] and WinPLOTR software has been used to prepare the PXRD illustrations.[45] Estimation and refinement of the unit cell parameter from the PXRD diagrams have been performed using the FOX and fullprof softwares.[46,47]

SINGLE CRYSTAL X-RAY CRYSTALLOGRAPHY Crystallographic data of 3-ASA were collected at 150 K on a small single crystal of $0.05 \times 0.02 \times 0.02$ mm^3, on a R-Axis Rapid Rigaku MSC diffractometer with monochromatic Cu-Kα radiation (λ = 1.54178 Å) and a curved image plate detector. At 150 K, the full sphere data collection was performed using φ scans and ω scans. The unit cell determination and data reduction were performed using the crystalclear program suite[48] on the full set of data. The crystal structure was solved by direct methods and successive Fourier difference syntheses with the SHELXS-97 program.[49] The refinements of the crystal structure were performed on F^2 by weighted anisotropic full-matrix least squares methods using the SHELXL97 program.[49] The different pieces of software were used within the the OLEX2 package.[44] Absorption correction was applied by multiscan methods using the scaling program implemented in crystalclear suite software. All non-H atoms were refined anisotropically. The positions of H atoms were deduced from the Fourier difference map and refined but treated with isotropic displacement parameters, corresponding to 1.2 to 1.5 the Ueq of the parent atom they are linked to.
Crystallographic data have been deposited in the Cambridge Crystallographic Data Centre (CCDC number 1056289). Copies of these data can be obtained free of charge from the Director, CCDC, 12 Union Road, Cambridge, CB2 1EZ, UK (fax: +44 1223 336 033; e-mail: deposit@ccdc.cam.ac.uk or http://www.ccdc.cam.ac.uk/data_request/cif

POWDER COMPOSITION In case of cocrystallization experiments, the content of powders in ASA and NCTA was determined by high performance liquid chromatography (HPLC) after dissolution in acetone:DMSO or in acetonitrile depending on ASA isomers. An Agilent 1200 system (Agilent Technologies) equipped with a diode array detector (DAD, G1315A), an autosampler (G1329A) and a Chemstation software was used with a ZORBAX Eclipse Plus C18 column (4.6 x 100 mm, 3.5 μm, Agilent Technologies) kept at 25°C.

Elution was performed under isocratic conditions with phosphate buffer (20 mM, pH 3.3) and acetonitrile (35:65 vol %) at 1.2 mL/min flow rate. Aminosalicylates and NCTA were quantified at 300 nm and 263 nm respectively from calibration curves obtained in the range of 0.4 – 5 mg/mL. The quantification of species in produced powders allowed for calculating the recrystallization yield of each component, defined as the ratio between the collected and the processed amounts.

FTIR SPECTROSCOPY Interactions between aminosalicylates and nicotinamide that would evidence cocrystal formation were assessed by infrared spectroscopy. ATR-FTIR spectra on diamond crystal (GoldenGate) were recorded with NEXUS 870 FTIR ESP spectrometer from Nicolet (Madison, USA) equipped with a liquid nitrogen cooled mercury-cadmium-telluride detector. Analyses were performed at room temperature between 800 and 4000 cm^{-1} with a resolution of 2 cm^{-1} and 100 scans. Physical mixtures of aminosalicylates and NCTA single-recrystallized by CO_2 were prepared for comparison.

NMR SPECTROSCOPY Liquid state NMR experiments were carried out on a Bruker Avance 400 MHz (9.39 T) SB spectrometer (Wissembourg, France) using a 5 mm QNP probe (1H/19F-13C-31P) equipped with Z-gradients. 1H NMR and ^{13}C NMR spectra were recorded at 25°C, operating at 400MHz for proton and at 100MHz for carbon. A single pulse sequence (zg) was used to record proton spectra: 90° pulse width of 15 µs, repetition time of 2s, Lorentzian line broadening of 0.3 Hz. A power gated decoupling scheme was used to record ^{13}C liquid state NMR (zgpg): 90° pulse width of 14 µs, repetition time of 5s, Lorentzian line broadening of 2 Hz. Samples were dissolved in acetone-d6/DMSO-d6 (90:10). Chemical shifts (δ) are quoted in parts per million and are calibrated relative to solvent residual peaks. The software for acquisition and processing is Topspin 2.1 (Bruker)

Results and discussion

Single component recrystallization: morphological variation and polymorphism assessment

The CO_2-antisolvent crystallization technique was first applied to pure components in conditions of solvent and concentration summarized in Table 1. Morphology and particle size distribution of products before and after CO_2 processing are shown in Fig. 2, whereas PXRD spectra are given in Fig. 3.

Before detailing individual results, a general comment is that GAS recrystallization yielded products of completely different morphologies, excepted for the 4-ASA.

5-ASA RECRYSTALLIZATION. Recrystallized 5-ASA was recovered with a yield of 48%, indicating a significant residual solubility in the CO_2 + acetone:DMSO (70:30) mixture. Whereas the raw material consisted in off-white to grey expanded cottony powder, the CO_2 recrystallized 5-ASA was a fine beige to tan powder. The d_{90} issued from the volume % - distribution analysis decreased from 117 µm for the raw 5-ASA to 70 µm for the recrystallized powder. The size distribution pattern initially trimodal turned into nearly unimodal (Figure 2), leading to a change in polydispersity index (span) from 4.4 to 1.5. As seen as well in figure 2, the particle shape changed significantly from needles (length up to 100 µm and width around 10 µm) to small and thin platelets aggregated in spheres of 10 µm in diameter like sandroses. The CO_2-antisolvent crystallization technique allowed thus the micronization of particles and the spheronization of aggregates from needle-like to spherical sandroses. Crystal shape is a critical parameter in pharmaceutical industries since it affects the flow properties and the compaction of powders. Hence, production of spherical crystals has gained great attention and importance in the last 20 years. More specific to salicylic derivatives, the transformation of tetragonal and prism-shaped acetylsalicylic acid crystals into spherical agglomerates significantly improved the API flowability and compactibility[50], an improvement underlined as well by Vinita et al. about 5-ASA co-agglomerates.[51] Di Pretoro et al. studied the impact of needle-shaped crystals on wet and solid-lipid extrusion processes, taking 5-ASA as model compound.[33] In order to achieve robust extrusion processes, a micronization step by air-jet milling was introduced prior extrusion to reduce the API size, change its morphology and produce more isometric particles. By producing micron-sized and spherical aggregates, the CO_2-antisolvent technique could be therefore a valuable process for shaping 5-ASA. It is worth noting that agglomerates can be further downsized by changing operating conditions. For instance, higher stirring and CO_2 introduction rates (900 rpm and 34 g/min, respectively) yielded crystals of similar spherical shape but of 5 µm diameter instead of 10 µm.
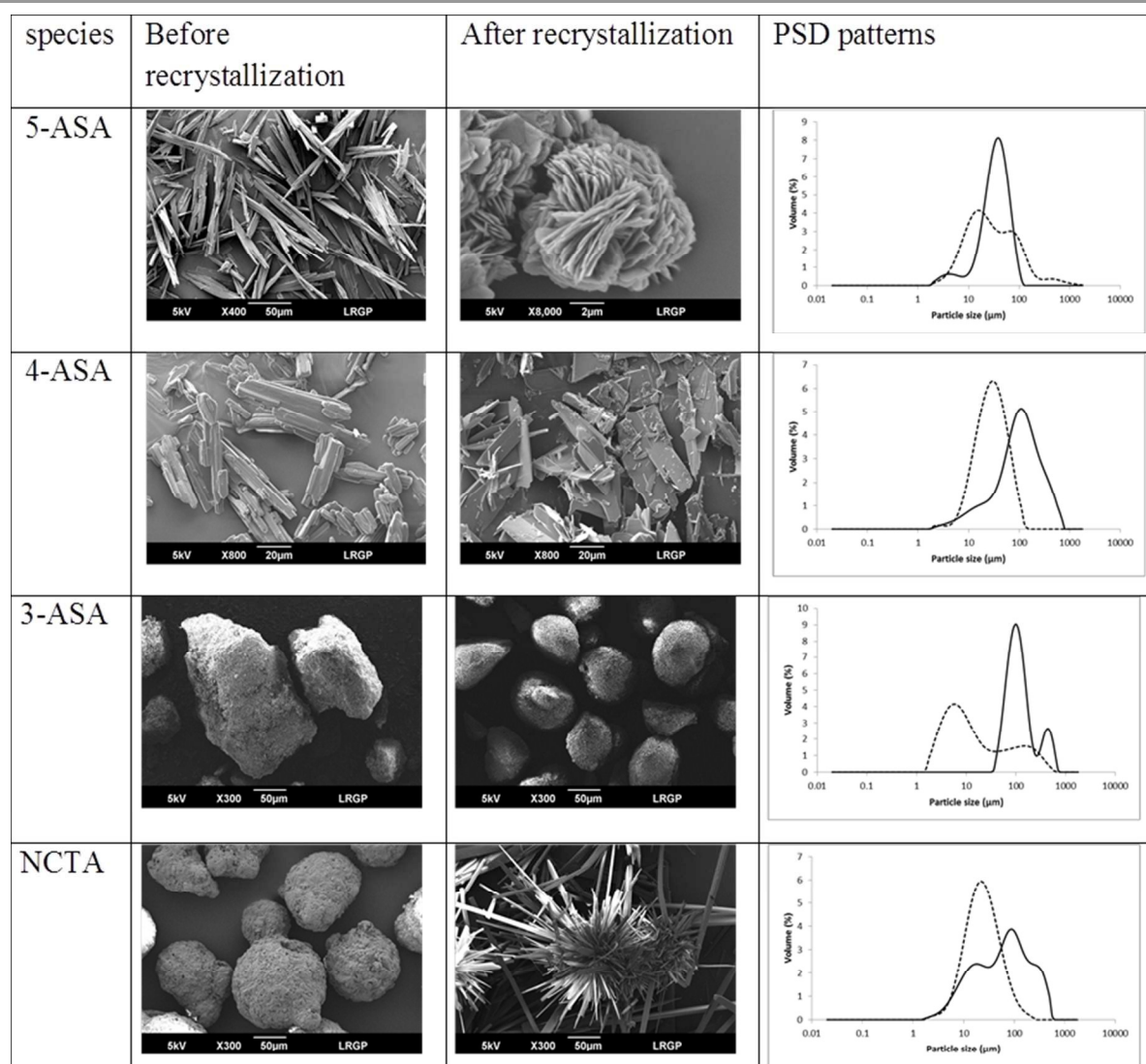
Fig. 2. SEM photographs and PSD patterns of particles before and after CO_2 recrystallization. For PSD: raw materials (dotted lines) and recrystallized products (plain lines).

Flow properties of the produced powder were more precisely evaluated through the Carr Index and the Hausner ratio. Before processing, the raw powder presented a CI of 46% and a H of 1.8, these values being consistent with those reported by Di Pretoro[33] or by Roy[6] for needle-shaped APIs. These values are indicative of a cohesive powder of poor flowability (CI > 25%, H > 1.25). After CO_2 recrystallization, the obtained 5-ASA showed a Carr Index of 30% and a Hausner ratio of 1.4, which indicated more free-flowing particles even though the final powder remained rather cohesive. These values were comparable to those obtained for 5-ASA micronized by jet milling (H = 1.4 and CI = 30.9%).[33]

Regarding crystal form, the obtained powder exhibited exactly the same PXRD pattern than the raw material, with characteristic 2θ values of 7.5°, 15.1° and 16.5° (Fig. 3). CO_2 recrystallization did not induce any change in the crystal lattice, so that the initial crystallographic form was preserved. No change in the FTIR spectrum was noticed either (not shown).
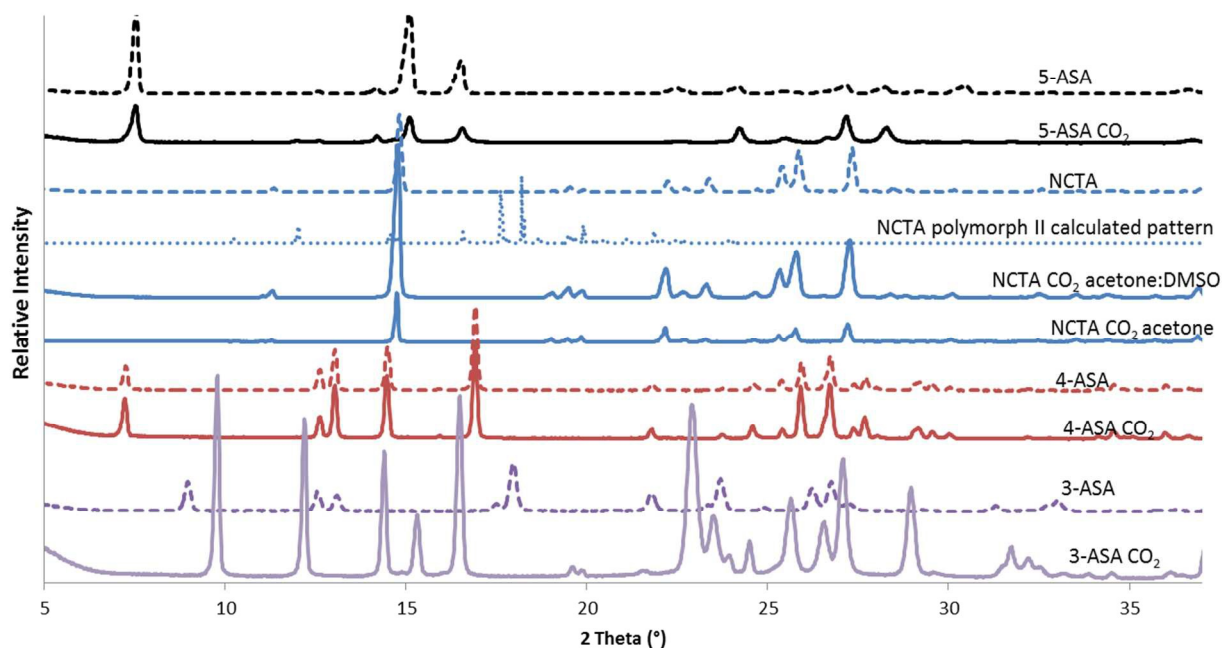
Fig. 3. PXRD patterns of raw (dotted lines) and CO_2-produced (lines) materials, showing that the crystal lattice is preserved for most compounds. Only 3-ASA is modified. NCTA has been recrystallized in pure acetone and in acetone:DMSO (70:30 vol%) mixture. The theoretical PXRD pattern of the form II of NCTA P2/n polymorphic species is also given.

4-ASA RECRYSTALLIZATION 4-ASA was recovered with a yield as high as 76%, indicating that its residual solubility in the CO_2 + acetone mixture is lower than that of 5-ASA in CO_2 + acetone:DMSO. The change of 4-ASA morphology after CO_2 processing was less impressive than for 5-ASA. The white expanded cottony powder transformed into off-white and more free-flowing powder. Commercial 4-ASA is a crystalline powder where crystallites look like tetragonal single crystals with plane boundaries, whereas the CO_2-recrystallized product was made of platelets thinner but larger than raw particles (Fig. 2). The d_{90} varied from 70 μm to 340 μm, the span from 2.0 to 4.4 and the size distribution pattern, nearly unimodal for the supplied 4-ASA, turned into a rather trimodal pattern that evidenced that the CO_2-product was more polydispersed than the raw material. However, the Hausner ratio and Carr Index varied only slightly from the commercial to the reprocessed powder (1.8 to 1.7 and 42% to 40% respectively) indicating similar flowability. Regarding crystal organization, FTIR spectra were identical and PXRD patterns were exactly the same with characteristic 2θ values of 7.2°, 12.6°, 13°, 14.5°, 16.9°, 25.9° and 26.7° (Fig. 3), indicating that no polymorphic transformation occurred. Hence, for this isomer, recrystallization by CO_2 did not yield significant modification or improvement.

3-ASA RECRYSTALLIZATION Raw 3-ASA is a grey rather cottony powder. Recrystallization of 3-ASA from an acetone:DMSO (90:10) solution yielded a very fine brownish-grey powder. The recovery yield of 44% indicates a rather high

3-ASA residual solubility in the CO_2+acetone:DMSO mixture. The recrystallized particles were rather spherical, 50 to 100 μm in diameter, made of aggregated micrometric crystals. On contrary, raw 3-ASA consisted in micrometric crystal agglomerates with no particular shape. Hence, CO_2 recrystallization yielded crystals with different morphology.

The size distribution pattern was bimodal for both the raw and recrystallized products (Fig. 2). However, the d_{90} varied from 217 μm to 402 μm and the span from 18.6 to 2.9 for the supplied 3-ASA and the produced powder respectively. The CO_2 recrystallized powder consisted then in larger particles but far less polydispersed in size than the raw material. The spheronization and better macroscopic behaviour advocated measurements of flow properties but low produced amount and insufficient availability of raw 3-ASA did not allow them.

Contrary to other isomers, recrystallized 3-ASA exhibited a FTIR spectrum slightly different from that of the raw material especially in the 1500-1700 cm^{-1} region (FTIR spectra provided in SI, Fig. S1). This part of spectrum was less complex for the CO_2 recrystallized 3-ASA than for the raw material, which might indicate fewer intermolecular interactions. However, primary amines have been shown to be very reactive with CO_2, forming carbamates[52] that are evidenced by bands corresponding to C=O and N-C stretching in the range 1700-1640 cm^{-1} and at 1540 cm^{-1} respectively. Since aminosalicylates possess an amine, and since recrystallized 3-ASA FTIR spectrum was different from that of raw 3-ASA in that particular 1500-1700 cm^{-1} region, the potential formation of carbamate was more deeply checked. Both raw and

recrystallized 3-ASA were analyzed by proton, carbon, HMBC and HMQC NMR (carbon NMR spectra provided in SI, Fig. S2). NMR analysis evidenced no chemical modification for the recrystallized 3-ASA, thus excluding carbamate formation. In addition to FTIR spectrum modification, PXRD pattern largely differed as well (fig. 3). The characteristic 2θ values for raw 3-ASA were 8.9°, 17.9°, 23.7°, 26.2° and 26.8° whereas those of recrystallized 3-ASA were 9.8°, 12.2°, 14.4°, 16.5°, 22.9° and 27.1°. To authors's best knowledge, no crystal structure of 3-ASA was deposited at the CCDC (CSD search april 2015).

3-ASA (**1**) crystallized in the monoclinic $P2_1/c$ space group. The asymmetric unit consists in one independent molecule (fig.4), crystal data and details concerning the X-ray diffraction experiment and refinement of the single crystal structures are given in table S1.
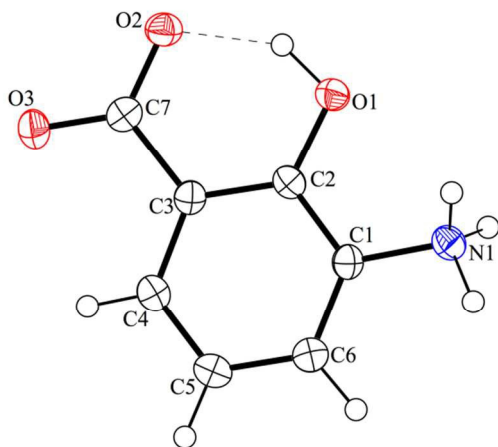

Fig. 4. Thermal ellipsoïd drawing (30% probability) of **1** showing the labelling scheme.

The whole molecule is nearly planar as the maximum deviation of non-H atoms from the aromatic plane is observed at 0.189 Å for O3. This slight deviation is a consequence of a small tilt of 5.2° between the aromatic ring and the carboxylate planes. The aromatic character of the C1-C6 ring is clearly verified by the C-C bond lengths that range from 1.378 Å to 1.403 Å (table S2). This planar conformation is stabilized by a strong intra-molecular H-bond between O2 and H1 (see table S3 and fig. 4). According to the positions found for the H atoms, the 3-ASA molecule has to be a zwitterion. Furthermore, the zwitterionic structure is confirmed, on one hand by the long C1-N1 bond (1.453 Å), which is found in the expected range for single carbon ammonium bond (from 1.445Å to 1.482 Å), and longer than the expected value for a partially π delocalized C_{ar}-NH_2 bond (from 1.336 Å to 1.421Å)[53] and, on the other hand, by the two quasi - equivalent C7-O2 and C7-O3 respectively found at 1.283 Å and 1.264 Å that lie in the expected range for a carboxylate anion (table S2). The crystal packing cohesion is ensured by a 2D network of charge-assisted hydrogen bonds between the ammonium and the carboxylate moiety within the **bc** plane and by weaker Van der Waals interactions of C-H / π type in the third direction (table S3).

Crystal lattices parameters have also been estimated from powder X-ray diffraction analysis for both raw and CO_2 recrystallized 3-ASA. The cell parameters have been found and refined by the profile matching method[54] and valued to a = 10.351(2) Å, b = 4.515(1) Å, c=14.783(2) Å, β = 107.28(1)° and a = 4.122(1) Å, b = 11.584(1) Å, c = 14.546(1) Å, β = 92.22(1)° corresponding to the unit cell volumes of V = 659.7(2) Å^3 and V = 694.1(1) Å^3 for the raw and the CO_2 recrystallized 3-ASA respectively (see fig. S3).

The raw 3-ASA crystal cell parameters estimated from PXRD analysis match well those determined by single crystal X-ray crystallography as the slight differences can be attributed to temperature effects (table S1). Thus, the cell parameters obtained by the same PXRD analysis on the yielded CO_2 recrystallized 3-ASA can be considered with a good level of confidence.

These results evidence that the yielded crystal is a polymorph in the same monoclinic $P2_1/c$ space group, but of lower density. This decreasing density might be indicative of a unionized neutral form. Although more thorough crystallographic investigations should be carried out to confirm the non-zwitterionic form, as for instance single crystal X-ray diffraction, the CO_2 antisolvent recrystallization process has however afforded the obtaining of a new polymorph.

NCTA RECRYSTALLIZATION For NCTA, the CO_2-recrystallization yielded a product of worse characteristics than the raw material. The initial spherical particles were transformed into large needles (fig. 2) so that at macroscopic scale, the commercial fine and free-flowing powder turned into a highly expanded and hardly flowing product. Only its white colour did not change. The d90 issued from the volume % - distribution analysis varied from 68 µm to 295 µm, the span increased from 2.4 to 4.2, and the size distribution pattern varied from an almost unimodal shape to a rather trimodal one (Fig. 2). The resulting crystals had worse flowability properties but in a slighter extend than expected (H and CI values increased from 1.1 to 1.2 and from 11% to 14% respectively). The recovery yield was 28% that showed the nicotinamide was highly soluble in the CO_2 + acetone:DMSO (70:30) mixture. Nicotinamide is a compound that exhibits polymorphism.[55] PXRD patterns in figure 3 evidence that the recrystallization products, obtained either from pure acetone or from acetone:DMSO, exhibit the same crystal lattice than the commercial product, i.e. the monoclinic $P2_1/c$ stable form. Characteristic 2θ values of 11.3°, 14.8°, 25.8° and 27.3°, clearly different than that of the known polymorphic P21/n form (17.6° and 18.2°)[55], confirmed that CO_2 did not realize the polymorphic conversion of NCTA. No change in FTIR spectrum was noticed either.

To sum up the CO_2 recrystallization topic of single components, isomerism caused a deep change in the recrystallization behaviour of APIs. Whereas recrystallization of 4-ASA did not induce major variation of the API morphology nor of the crystal structure, the process yielded

spherical particles with potential improved flowing properties in cases of 5-ASA and 3-ASA. Moreover, although neither a 4-ASA nor a 5-ASA polymorph was discovered, this process
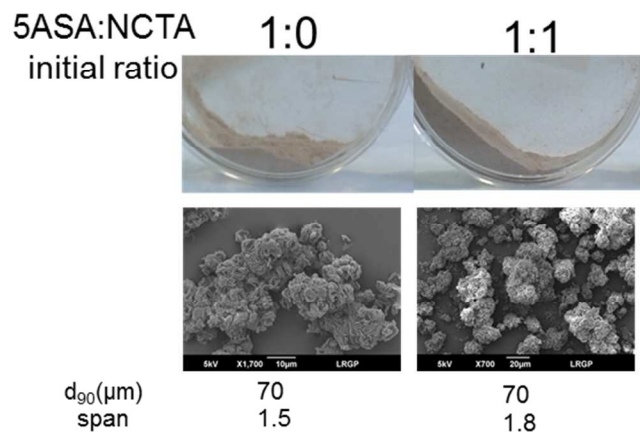

Fig. 5. Macroscopic appearance and SEM photographs of produced powders, from solutions with various 5-ASA:NCTA molar ratios. More NCTA in initial solution yields cotton-like and brightened products with more needle-shaped particles.

Recrystallization of ASA and NCTA mixture: production of cocrystals or homocrystals mixtures

Experiments were first focused on the fabrication of 5-ASA and NCTA cocrystals since no cocrystals were reported in literature for this isomer. The component ratio and the solvent were varied in attempts of promoting API-coformer interactions instead of API-API interactions. Cocrystallization was then carried out on 4-ASA and 3-ASA isomers that exhibited different inter/intra molecular interactions.

Mixtures of 5-ASA and NCTA were recrystallized from acetone:DMSO (70:30 vol%) solution since it was a successful combination for individual compound precipitation. Concentration of 5-ASA was set to 17 mg/mL whereas NCTA concentration was varied from 0 to 57 mg/mL in order to process different API:coformer ratios (5-ASA:NCTA molar ratio 1:0 to 1:4). Changing the API concentration was not an option since 17 mg/mL is close to 5-ASA solubility in the solvent mixture.

Upon the increasing NCTA concentration, powders evolved towards a more cotton-like product that brightened as well whilst SEM observations evidenced the simultaneous presence of needles and microscopic thin plates arranged in 10 μm diameter sand-roses (Fig. 5). The d_{90} characteristics of size distributions increased and the size distribution patterns became trimodal. All this morphological changes suggested homocrystal mixtures rather than cocrystals. This was confirmed by PXRD and FTIR. In both techniques, the produced powders exhibited the same patterns than single-processed components (Fig. 6 for PXRD pattern spectra, Fig. 7 for FTIR) indicating that no new interactions or new crystalline

converted 3-ASA into a new polymorph with a less compact crystal lattice that might indicate a neutral form of the API.

form were created. Powders were thus made of a physical mixture of 5-ASA and NCTA homocrystals rather than of cocrystals. In both FTIR and PXRD analyses, the intensities of peaks specific of NCTA and 5-ASA were found to vary with the processed NCTA concentration in solution, indicating that the NCTA:ASA ratio in the obtained powder varied accordingly. This was confirmed by HPLC quantifications (Fig. S4a): more NCTA in the initial solution yielded more NCTA in the final product which could also explain the macroscopic change of the powder towards more needles and cottony aspect (Fig. 5). Interestingly, in presence of increasing NCTA concentration, the recrystallization yield of 5-ASA was found to increase linearly (Fig. S4b), indicating that the addition of this extra species promoted the precipitation of the API.
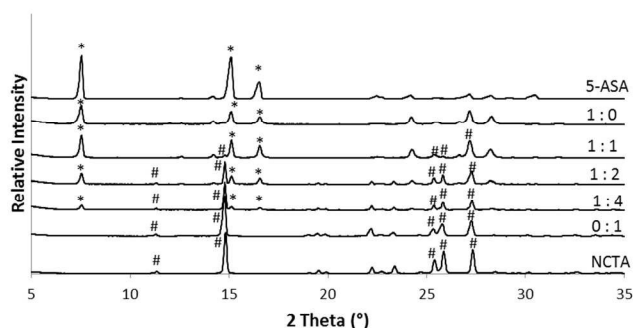

Fig. 6. PXRD patterns of pure 5-ASA, NCTA, and of products arising from CO_2 antisolvent recrystallization of solutions with various 5-ASA:NCTA ratios. Ratios 1:0 and 0:1 correspond to pure 5-ASA and NCTA, respectively. The main 2θ values characteristic from raw species are given: (*) 5-ASA and (#) NCTA.

In attempts of promoting cocrystallization intead of the homocrystallization obtained so far, the solvent - and consequently the solutes concentration- was modified, using acetone or DMSO only. Whatever the conditions, none of them realized the cocrystal fabrication.
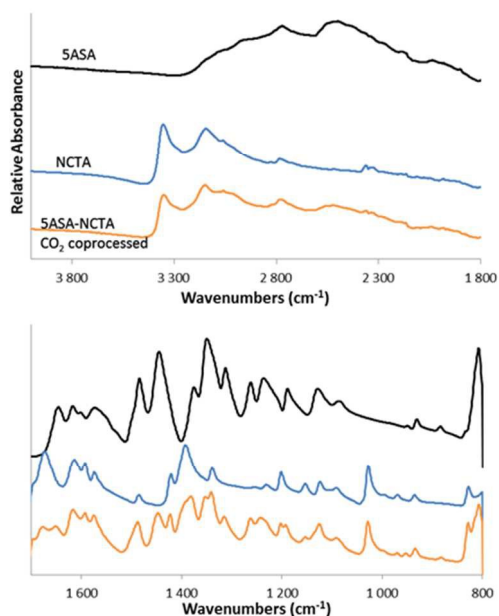
Fig. 7. ATR-FTIR spectra of pure 5-ASA, pure NCTA and 5-ASA:NCTA powder obtained from a 5ASA:NCTA solution of 17 and 32 mg/mL, respectively. Top: 4000-1800 cm^{-1} region; bottom: 1700-800 cm^{-1} region. Spectra do not evidence any interaction between 5-ASA and NCTA.
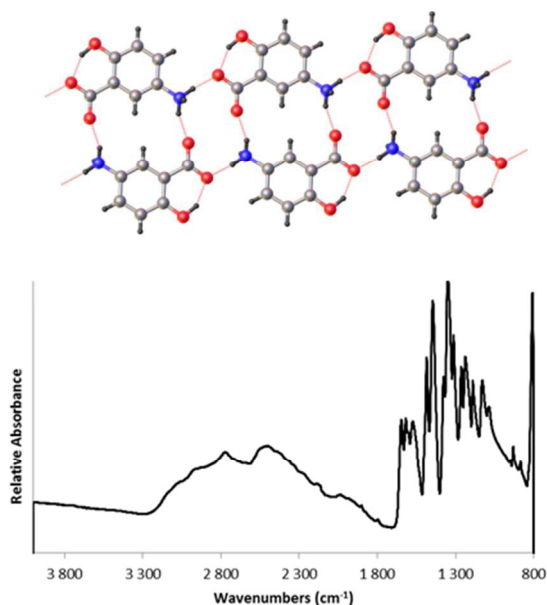

Fig. 8. (a:top) zwitterionic 5-ASA crystal packing; (b:bottom) ATR-FTIR spectrum of 5-ASA.

Homocrystallization preferably to cocrystallization suggests that interactions between API-API are stronger than that of API-coformer. In fact, contrary to many APIs that form cocrystals, 5-ASA is a zwitterionic molecule. Interestingly, zwitterionic species can be expected to be very potent cocrystal formers as charge-assisted hydrogen bonds are stronger than neutral hydrogen bonds.[56] Cocrystals from zwitterionic species have been fabricated, as for instance with amino acids[56,57], and even in a cocrystal, the zwitterionic form can be retained.[58]

The configuration of 5-ASA, with the hydroxyl and carboxyl groups in ortho position favours intramolecular hydrogen bonds, so that the crystal packing (Figure 8a) is a complex two-dimensional network of charge-assisted hydrogen bonds between amine and carboxyl groups.[59] The absence of the characteristics bands of amine around 3400 cm^{-1} and of carboxyl groups around 1600-1650 cm^{-1} in the ATR-FTIR spectrum (Figure 8b) is also indicative of the strong intermolecular interactions within the zwitterionic crystal.

Cocrystals of 5-ASA have not been reported in literature excepted as solvates[60] or salts.[61] Dealing with co-crystallizations of several substituted salicylic acids, among which 5-ASA, with 4-aminopyridine in a variety of solvents, Montis et al. concluded of the frequent unpredictability in the structure adopted by products when ionic forms are produced.[60] Most investigated pairs adopted the normal carboxylate ••• pyridinium synthon (carboxylic group of the salicylic acid and nitrogen group from the pyridine), excepted the 5-ASA that cocrystallized only as a 5-ASA:4-aminopyridine:pyridine solvate and adopted an alternative supramolecular synthon involving a coformer-solvent interaction. When crystallization was carried out in DMSO, no cocrystal was formed, confirming the primary role of the solvent into the cocrystal fabrication. Salts of mesalamine hydrochloride (5-ASA, HCl) with coformers such as α-amino acids and quercetine were reported.[61] In our own investigations where no cocrystal was obtained neither in DMSO nor in acetone:DMSO mixtures, NCTA was obviously unable to compete with the strong self interactions of 5-ASA, and the use of compressed CO_2 did not allow forcing NCTA to disrupt the 5-ASA hydrogen network neither.

As seen in Figure 8a, the amine position is critical for the interactions with carboxyl groups. Hence, the variation of NH_2 position might prevent these interactions from occurring, giving thus opportunities for the chemical groups to interact with the coformer and form cocrystals. Contrary to 5-ASA, 4-ASA exists as a unionized neutral form.[36] Incidentally, the formation of cocrystals with 4-ASA has been only recently screened and the preparation of 4-ASA:NCTA cocrystal and its hydrate by evaporation and co-grinding has been reported.[36,38] Contrarily, 4-ASA did not form any cocrystal with 4-aminopyridine in DMSO or pyridine.[60]

Solution of 4-ASA and NCTA in acetone was processed by the CO_2-recrystallization technique using an equimolar mixture of 4-ASA and NCTA which is the reported cocrystal stoichiometry.[36] PXRD analysis (Fig. 9) confirmed that a cocrystal was formed since the pattern exhibited specific peaks at 2θ values of 6°, 12°, 15.1° and 26.8° that were not in the patterns of single processed materials. Furthermore, this pattern matched that of the reported 4-ASA:NCTA cocrystal evidencing the same 1:1 stoichiometry as well.[38] Presence of a cocrystal hydrate in the powder was detected, which was consistent with the ability of this cocrystal to spontaneously catch atmospheric water to form the hydrated cocrystal.[38] The

ATR-FTIR analysis (Fig. 10) confirmed the creation of interactions between 4-ASA and NCTA, and showed that the NH_2 group of both components was implied in the cocrystal arrangement whereas only the C=O of NCTA was engaged into interactions. It is worth noting that the modifications reported herein did not appear in the physical mixture of recrystallized species. The presence of only cocrystals in the powder was confirmed by HPLC that indicated a similar molar amount of NCTA and 4-ASA. Since none of the species was in excess and according to the 1:1 cocrystal stoichiometric ratio, the powder was almost pure in cocrystals. By regards of the amount produced, the cocrystallization yield was as high as 60%. The obtained powder was a white and fine powder whose Hausner ratio of 1.5 and Carr Index of 33.2% indicated rather good flowing characteristics. The size distribution exhibited a bimodal pattern with a d_{90} of 175 µm and a span of 2.
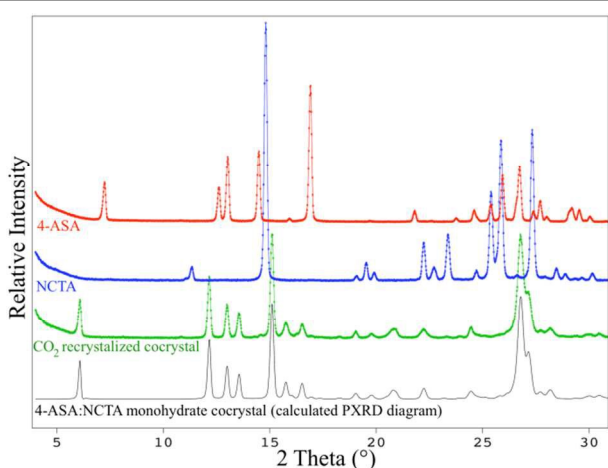

Fig. 9. PRXD diagrams of 4-ASA, NCTA, and4-ASA:NCTA monohydrate cocrystal produced by CO_2 recrystallization and simulated pattern of the cocrystal. The theoretical pattern has been calculated from the single crystal data found in the CSD[36] and refined by profile matching (LeBail method) to better estimate the room temperature cell parameter as the angle crystal data were performed at 100K. The different pattern of coprocessed 4-ASA+NCTA mixture evidences the formation of a cocrystal.
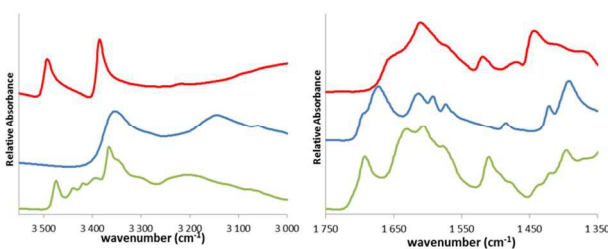

Fig. 10. Experimental ATR-FTIR spectra of powders produced by CO_2 recrystallization: 4-ASA:NCTA cocrystal (green), 4-ASA single recrystallized (red) and NCTA single recrystallized (blue). Spectra are highlighted for the NH_2 region (3550-3000 cm^{-1}) and for the C=O region (1750-1350 cm^{-1}) of both 4-ASA and NCTA. The CO_2 processed 4-ASA:NCTA solution yields a product whose spectrum largely differs from the overlapping of both individual species spectra.

3-ASA is another positional isomer of 5-ASA and 4-ASA. Contrary to others, this compound has no pharmaceutical use

and there is almost no data on 3-ASA excepted for its thermal behaviour[62] or cytotoxicity.[63,64] 3-ASA and NCTA were coprocessed in acetone:DMSO, 90:10 or 70:30 vol %, at concentrations in the range of 10 mg/mL and 20 mg/mL for 3-ASA and NCTA respectively, in both solvent mixtures (Table 1). The 70:30 mixture yielded only few particles that were however collected and analyzed, whereas a higher yield of 19% was obtained with the 90:10 mixture. FTIR spectra (Fig. 11) and PXRD patterns (Fig. 12) of produced powders exhibited the same characteristics than that of CO_2 recrystallized new polymorph of 3-ASA, and of NCTA when present. NCTA attributes were clearly visible in the powder produced form the 90:10 acetone:DMSO. Quantification by HPLC confirmed that the content of NCTA in powders increased with the increasing acetone ratio in the processed solution. Behaviours of 5-ASA and 3-ASA were similar, so we suspected that 3-ASA might be a zwitterionic molecule as well. This hypothesis is supported by the noticeable absence of NH_2 vibration bands in the 3000-3500 cm^{-1} region of FTIR spectra. 3 and 5-ASA present higher nucleophilic behaviours than 4-ASA for which the total delocalization of the amine nonbonding electronic pair can occur on the whole molecule.
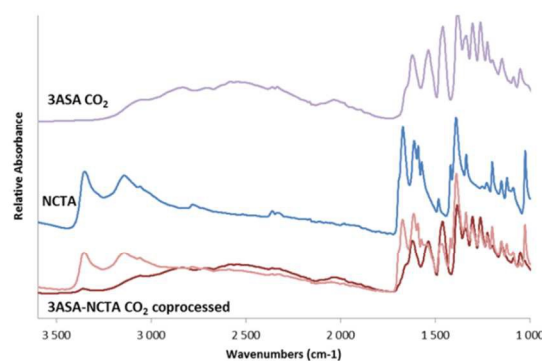
Fig. 11. ATR-FTIR spectra of coprocessed 3-ASA+NCTA mixture by CO_2 recrystallization from acetone:DMSO 70:30 (dark red) or acetone:DMSO 90:10 (bright pink). Spectra of NCTA and 3-ASA are given for comparison. No interaction between API and coformer is noticeable.
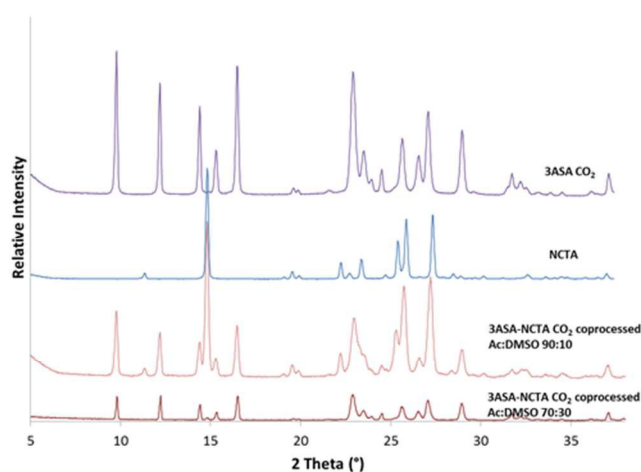
Fig. 12. PXRD patterns of coprocessed 3-ASA+NCTA mixture by CO_2 recrystallization from acetone:DMSO 70:30 (dark red) or acetone:DMSO 90:10 (bright pink). Spectra of NCTA and 3-ASA are given for comparison. Patterns confirm that coprocessed 3-ASA+NCTA is a physical mixture of the new 3-ASA polymorph and NCTA.

Conclusion

Recrystallization by CO_2-antisolvent technique was investigated as a new way to produce aminosalicylate crystals and cocrystals. When carried out from solutions of pure compounds, the process led to a dramatic change in product morphology. Single recrystallized 3-ASA and 5-ASA became micrometric spherical crystals, thus probably exhibiting superior flowing properties compared to the raw materials. However, the GAS process did not induce any change in the 5-ASA crystal lattice whereas it produced a new 3-ASA polymorph of similar monoclinic $P2_1/c$ space group but of lower density than the raw 3-ASA. Morphology variation was merely noticeable on 4-ASA that did not undergo any change of crystal lattice either. The lack of polymorphism of this molecule was already underlined by Cherukuvada et al.[36]

Based on their complementary hydrogen bond donor and acceptor sites, aminosalicylates and nicotinamide were promising candidates for the production of cocrystals, although only cocrystal with 4-ASA was yet reported. API isomerism induced deep changes in the obtained product. Whereas a cocrystal and its hydrate were produced from 4-ASA, the processing of 5-ASA or 3-ASA yielded physical mixtures of homocrystals. More specifically, from 5-ASA+NCTA mixtures, the CO_2 antisolvent technique did not succeed at producing a cocrystal whatever the processed conditions of increasing coformer concentration or varying solvent and consequently species concentration. Produced powders were thus mixtures of homocrystals whose morphology and composition varied according to the initial processed NCTA content. Despite the multiple hydrogen-bonding facilities provided by the various

functional groups, 5-ASA molecules did not accommodate the coformer in their network, which indicated that the CO_2 envisaged technique was not able to disrupt the strong inter se interactions provided by the zwitterionic 5-ASA. Similarly, 3-ASA, although its zwitterionic character is not proven so far, did not form any cocrystal with NCTA. Only their 4-ASA analogue led to a cocrystal, of same stoichiometry and hydrogen bonding network as the 4-ASA:NCTA cocrystal recently obtained by classical routes of grinding and evaporation.

Overall results confirm that the presence of chemical groups susceptible to form molecular interactions in API and coformer molecules is not sufficient to fabricate cocrystals. In reference to the different isomers CO_2 processed in this work, it appears that positions of functional groups are critical for the potentiality to interact with a coformer or for forming a polymorph.

Acknowledgements

Note

Authors declare no competing financial interest.
Electronic Supplementary Information (ESI): ATR-FTIR spectra of raw 3-ASA and CO_2 recrystallized 3-ASA, carbon NMR spectra of raw 3-ASA and CO_2 recrystallized 3-ASA, influence of NCTA on 5-ASA crystallization, crystal data and details concerning the X-ray diffraction experiment and refinement of the single crystal structures of raw 3-ASA (1), bond lengths for 1, hydrogen bonds for 1, and profile matching of raw and CO_2 recrystallized 3-ASA. For ESI, see DOI: xxxx

Abbreviations

API, active pharmaceutical ingredient; ASA, amino salicylic acid; NCTA, nicotinamide; DMSO, dimethylsulfoxide; GAS, gaseous antisolvent; HPLC, high performance liquid chromatography; CI, Carr Index; H, Hausner ratio; TD, tapped density; BD, bulk density.

References

1   N. Shan, M. L. Perry, D. R. Weyna and M. J. Zaworotko, *Expert Opin. Drug Metab. Toxicol.*, 2014, **10**, 1255–1271.
2   J. Lu and S. Rohani, *Curr. Med. Chem.*, 2009, **16**, 884–905.
3   D. J. Good and N. Rodríguez-Hornedo, *Cryst. Growth Des.*, 2009, **9**, 2252–2264.
4   N. Schultheiss and A. Newman, *Cryst. Growth Des.*, 2009, **9**, 2950–2967.
5   N. A. Meanwell, in *Annual Reports in Medicinal Chemistry*, ed. J. E. Macor, Academic Press, 2008, vol. 43, pp. 373–404.
6   WO2009116055 (A1), 2009.

7   J. Lu and S. Rohani, *Org. Process Res. Dev.*, 2009, **13**, 1262–1268.
8   S. Ando, J. Kikuchi, Y. Fujimura, Y. Ida, K. Higashi, K. Moribe and K. Yamamoto, *J. Pharm. Sci.*, 2012, **101**, 3214–3221.
9   A. Sarkar and S. Rohani, *J. Pharm. Sci.*, 2015, **104**, 98–105.
10 M. Kalani and R. Yunus, *Int. J. Nanomedicine*, 2011, 1429.
11 P. Sheth, H. Sandhu, D. Singhal, W. Malick, N. Shah and M. Serpil Kislalioglu, *Curr. Drug Deliv.*, 2012, **9**, 269–284.
12 C. Roy, D. Vrel, A. Vega-González, P. Jestin, S. Laugier and P. Subra-Paternault, *J. Supercrit. Fluids*, 2011, **57**, 267–277.
13 M. Moneghini, I. Kikic, D. Voinovich, B. Perissutti, P. Alessi, A. Cortesi, F. Princivalle and D. Solinas, *Eur. J. Pharm. Biopharm.*, 2003, **56**, 281–289.
14 R. Bettini, L. Bonassi, V. Castoro, A. Rossi, L. Zema, A. Gazzaniga and F. Giordano, *Eur. J. Pharm. Sci.*, 2001, **13**, 281–286.
15 S.-J. Park, S.-Y. Jeon and S.-D. Yeo, *Ind. Eng. Chem. Res.*, 2006, **45**, 2287–2293.
16 H. J. Park, M.-S. Kim, S. Lee, J.-S. Kim, J.-S. Woo, J.-S. Park and S.-J. Hwang, *Int. J. Pharm.*, 2007, **328**, 152–160.
17 Y.-P. Chang, M. Tang and Y.-P. Chen, *J. Mater. Sci.*, 2008, **43**, 2328–2335.
18 A. Kordikowski, T. Shekunov and P. York, *Pharm. Res.*, 2001, **18**, 682–688.
19 C. Neurohr, A.-L. Revelli, P. Billot, M. Marchivie, S. Lecomte, S. Laugier, S. Massip and P. Subra-Paternault, *J. Supercrit. Fluids*, 2013, **83**, 78–85.
20 L. Padrela, M. A. Rodrigues, S. P. Velaga, H. A. Matos and E. G. de Azevedo, *Eur. J. Pharm. Sci.*, 2009, **38**, 9–17.
21 J. M. Tiago, L. Padrela, M. A. Rodrigues, H. A. Matos, A. J. Almeida and E. G. de Azevedo, *Cryst. Growth Des.*, 2013, **13**, 4940–4947.
22 G. R. Desiraju, *CrystEngComm*, 2003, **5**, 466–467.
23 G. He, C. Jacob, L. Guo, P. S. Chow and R. B. H. Tan, *J. Phys. Chem. B*, 2008, **112**, 9890–9895.
24 T. Jacobs, G. O. Lloyd, M. W. Bredenkamp and L. J. Barbour, *Cryst. Growth Des.*, 2009, **9**, 1284–1286.
25 E. Gagnière, D. Mangin, F. Puel, A. Rivoire, O. Monnier, E. Garcia and J. P. Klein, *J. Cryst. Growth*, 2009, **311**, 2689–2695.
26 Z. Q. Yu, P. S. Chow and R. B. H. Tan, *Cryst. Growth Des.*, 2010, **10**, 2382–2387.
27 T. Leyssens, N. Tumanova, K. Robeyns, N. Candoni and S. Veesler, *CrystEngComm*, 2014, **16**, 9603–9611.
28 S. Karki, T. Friščić and W. Jones, *CrystEngComm*, 2009, **11**, 470–481.
29 G. Margagnoni, C. Pagnini, F. Menasci, S. Festa and G. D. Fave, *Curr. Clin. Pharmacol.*, 2014, **9**, 84–90.
30 F. Daniel, P. Seksik, W. Cacheux, R. Jian and P. Marteau, *Inflamm. Bowel Dis.*, 2004, **10**, 258–260.
31 S. S. Dhaneshwar, *World J. Gastroenterol.*, 2014, **20**, 3564–3571.
32 J. Lehmann, *The Lancet*, 1946, **247**, 15–16.
33 G. Di Pretoro, L. Zema, A. Gazzaniga and P. Kleinebudde, *Powder Technol.*, 2015, **270**, 476–483.
34 A. Vega-Gonzalez, Subra-Paternault, P. and D. Vrel, *Proc. 8th Int. Symp. Supercrit. Fluids*, 2006.
35 D. Hu, L. Liu, W. Chen, S. Li and Y. Zhao, *Int. J. Mol. Sci.*, 2012, **13**, 6454–6468.
36 S. Cherukuvada, G. Bolla, K. Sikligar and A. Nangia, *Cryst. Growth Des.*, 2013, **13**, 1551–1557.
37 R. Montis and M. B. Hursthouse, *CrystEngComm*, 2012, **14**, 5242–5254.
38 I. Sarcevica, L. Orola, S. Belyakov and M. V. Veidis, *New J. Chem.*, 2013, **37**, 2978–2982.

39 P. K. Goswami, R. Thaimattam and A. Ramanan, *Cryst. Growth Des.*, 2013, **13**, 360–366.
40 P. Grobelny, A. Mukherjee and G. R. Desiraju, *CrystEngComm*, 2011, **13**, 4358–4364.
41 B. De Gioannis, P. Jestin and P. Subra, *J. Cryst. Growth*, 2004, **262**, 519–526.
42 A. E. Andreatta, L. J. Florusse, S. B. Bottini and C. J. Peters, *J. Supercrit. Fluids*, 2007, **42**, 60–68.
43 P. Subra, C.-G. Laudani, A. Vega-González and E. Reverchon, *J. Supercrit. Fluids*, 2005, **35**, 95–105.
44 O. V. Dolomanov, L. J. Bourhis, R. J. Gildea, J. A. K. Howard and H. Puschmann, *J. Appl. Crystallogr.*, 2009, **42**, 339–341.
45 T. Roisnel and J. Rodríquez-Carvajal, *Mater. Sci. Forum*, 2001, **378-381**, 118–123.
46 V. Favre-Nicolin and R. Černý, *J. Appl. Crystallogr.*, 2002, **35**, 734–743.
47 J. Rodríguez-Carvajal, *Phys. B Condens. Matter*, 1993, **192**, 55–69.
48 Rigaku, 1998.
49 G. M. Sheldrick, *Acta Crystallogr. A*, 2008, **64**, 112–122.
50 H. Göczõ, P. Szabó-Révész, B. Farkas, M. Hasznos-Nezdei, S. F. Serwanis, K. Pintye-Hódi, P. Kása Jr., I. Erõs, I. Antal and S. Marton, *Chem. Pharm. Bull. (Tokyo)*, 2000, **48**, 1877–1881.
51 K. Vinita, G. Shrikant, A. Chavardol and K. Moharir, *Pharm. Lett.*, 2011, **3**, 212–219.
52 P. López-Aranguren, J. Fraile, L. F. Vega and C. Domingo, *J. Supercrit. Fluids*, 2014, **85**, 68–80.
53 F. H. Allen, O. Kennard, D. G. Watson, L. Brammer, A. G. Orpen and R. Taylor, *J. Chem. Soc. Perkin Trans. 2*, 1987, S1–S19.
54 A. Le Bail, *Powder Diffr.*, 2005, **20**, 316–326.
55 J. Li, S. A. Bourne and M. R. Caira, *Chem. Commun.*, 2011, **47**, 1530–1532.
56 A. Tilborg, G. Springuel, B. Norberg, J. Wouters and T. Leyssens, *CrystEngComm*, 2013, **15**, 3341.
57 N. Tumanova, N. Tumanov, K. Robeyns, Y. Filinchuk, J. Wouters and T. Leyssens, *CrystEngComm*, 2014, **16**, 8185–8196.
58 J. Hernández-Paredes, A. L. Olvera-Tapia, J. I. Arenas-García, H. Höpfl, H. Morales-Rojas, D. Herrera-Ruiz, A. I. Gonzaga-Morales and L. Rodríguez-Fragoso, *CrystEngComm*, 2015.
59 Z. Banić-Tomišić, B. Kojić-Prodić and I. Širola, *J. Mol. Struct.*, 1997, **416**, 209–220.
60 R. Montis and M. B. Hursthouse, *CrystEngComm*, 2012, **14**, 7466–7478.
61 R. Dandela, G. GADDAMANUGU, A. K. Kruthiventi, R. Nagalapalli, J. S. Reddy, A. K. SOLOMON and G. S. Viswanadha, *Novel cocrystals / molecular salts of mesalamine to be used as improved anti-inflammatory drug*, Google Patents, 2012.
62 M. K. Rotich, B. D. Glass and M. E. Brown, *J. Therm. Anal. Calorim.*, 2001, **64**, 681–688.
63 C. Campregher, M. G. Luciani, P. Biesenbach, R. Evstatiev, A. Lyakhovich and C. Gasche, *Inflamm. Bowel Dis.*, 2010, **16**, 576–582.
64 E. Noble, L. Janssen and P. J. Dierickx, *Cell Biol. Toxicol.*, 1997, **13**, 445–451.

CrystEngComm Accepted Manuscript

Graphical abstract
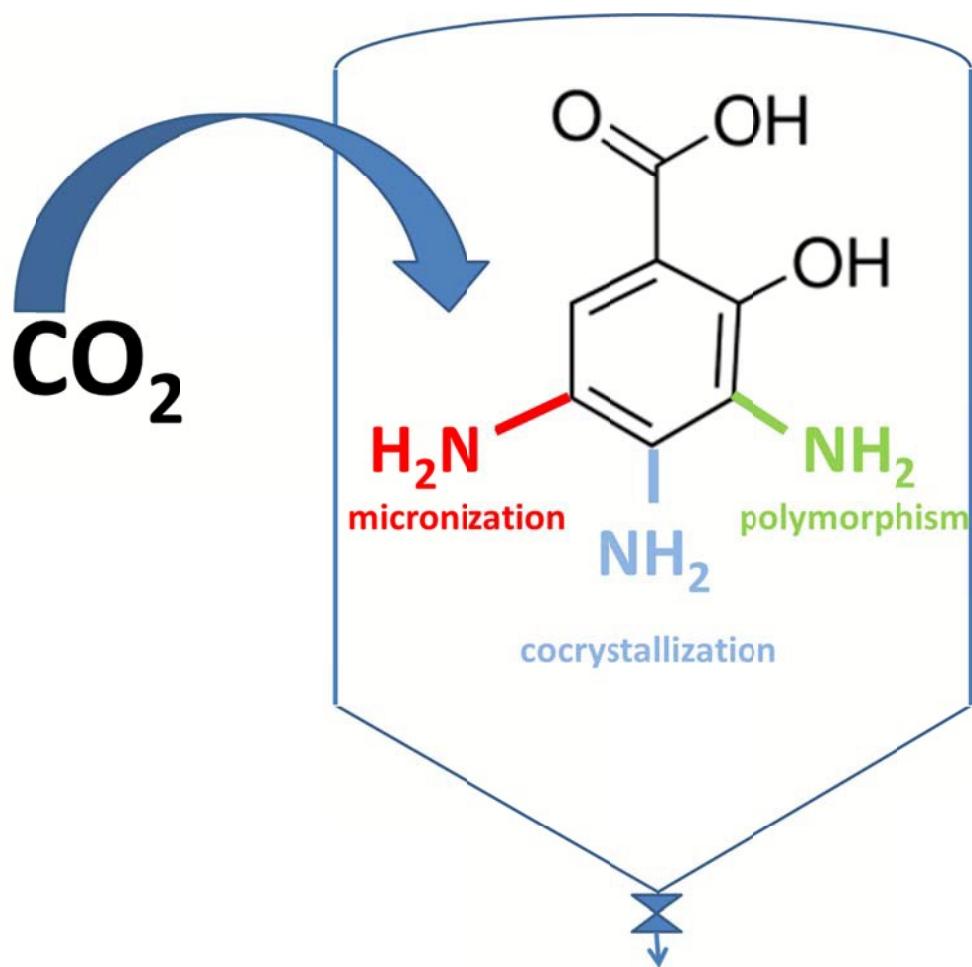
Textual abstract

Position of amine group in amino salicylic acid has a significant impact not only on the polymorph or cocrystal formation but also on crystal shape during CO_2-antisolvent crystallization.